



# Seasonal Trophic Dynamics of Sinking Particles in the Ulleung Basin of the East Sea (Japan Sea): An Approach Employing Nitrogen Isotopes of Amino Acids

Hyuntae Choi<sup>1</sup>, Jeomshik Hwang<sup>2</sup>, Yeongjin Ryu<sup>2</sup>, Guebuem Kim<sup>2</sup> and Kyung-Hoon Shin<sup>1\*</sup>

<sup>1</sup> Department of Marine Science and Convergence Technology, Hanyang University, Ansan, South Korea, <sup>2</sup> School of Earth and Environmental Sciences, Seoul National University, Seoul, South Korea

## OPEN ACCESS

### Edited by:

Toshi Nagata,  
The University of Tokyo, Japan

### Reviewed by:

Naohiko Ohkouchi,  
Japan Agency for Marine-Earth  
Science and Technology (JAMSTEC),  
Japan

Hilary G. Close,  
University of Miami, United States

### \*Correspondence:

Kyung-Hoon Shin  
shinkh@hanyang.ac.kr

### Specialty section:

This article was submitted to  
Marine Biogeochemistry,  
a section of the journal  
Frontiers in Marine Science

Received: 29 November 2021

Accepted: 22 March 2022

Published: 14 April 2022

### Citation:

Choi H, Hwang J, Ryu Y, Kim G and  
Shin K-H (2022) Seasonal Trophic  
Dynamics of Sinking Particles in the  
Ulleung Basin of the East Sea (Japan  
Sea): An Approach Employing  
Nitrogen Isotopes of Amino Acids.  
*Front. Mar. Sci.* 9:824479.  
doi: 10.3389/fmars.2022.824479

To identify the sources of organic matter, we examined nitrogen isotopes of the amino acids of sinking particles collected from July 2017 to March 2018 at 1000 and 2250 m in the Ulleung Basin, the southwestern part of the East Sea (Japan Sea). Compared to the 1000 m samples, sinking particles at 2250 m were found to contain more resuspended sediment and underwent more microbial degradation. The signature of microbial degradation was significant in winter-early spring than in late summer-autumn. The source amino acids of sinking particles showed a substantial decline in the isotopic ratio during winter at both depths, suggesting changes in the nitrogen source for primary production. The average trophic positions (TPs) of sinking particles were larger at 1000 m ( $2.3 \pm 0.3$ ) than at 2250 m ( $1.9 \pm 0.2$ ), indicating that organic matter was mainly derived from fecal pellet and other organic debris from heterotrophs. In winter, the average TPs of sinking particles at 1000 m decreased below 2.0, which probably reflects the minimum zooplankton grazing in the euphotic layer. Sinking particles near the seafloor (2250 m) showed lower TP values than those at 1000 m, demonstrating that sinking particles at 2250 m are affected by lateral transport, particularly during winter. Our results show that the nitrogen isotope ratios of amino acids in sinking particles reflect the seasonal dynamics of both nitrogen sources and trophic structure in the water column.

**Keywords:** amino acids, nitrogen isotopes, sinking particle, East Sea, Japan Sea

## INTRODUCTION

The East Sea (also known as the Japan Sea; hereafter, the East Sea) is a semi-enclosed marginal sea connected to the North Pacific Ocean and the Sea of Okhotsk. The Ulleung Basin (UB) is a highly productive region, located to the southwest of the East Sea (Yamada et al., 2005; Yoo and Park, 2009; Joo et al., 2014). According to Kwak et al. (2013), the annual primary production was  $273 \text{ gC m}^{-2} \text{ yr}^{-1}$  (*in situ*) and was exported largely (53.9%) from the euphotic layer in the UB region. High productivity is maintained even in summer because of the shallow surface mixed layer, allowing a more upward supply

of nutrients (Kwak et al., 2013). Physicochemical conditions cause seasonally varying phytoplankton community compositions (Choi et al., 2013).

The East Sea experienced a decrease in primary productivity from 2003 to 2012 (Joo et al., 2014). Increased surface seawater temperature (Joo et al., 2014) may provide favorable conditions for smaller phytoplankton (< 2  $\mu\text{m}$ ) occupying 23.6% of the total annual primary productivity, which increases to 34.9% in summer (Joo et al., 2017). The relative proportion of smaller particles can influence the heterotrophic protozoan population (Yang et al., 2009; Park et al., 2016a) and the extent of microbial degradation of the sinking organic matter (Yamaguchi and McCarthy, 2018). Such changes in the trophic structure of planktonic ecosystems influence biological pump efficiency, resulting in biogenic particles being mostly remineralized in the upper water column (Onodera et al., 2015). Time-series sediment traps have been deployed in the mesopelagic (1000 m) and bathypelagic (2000–2300 m) layers of the East Sea to understand spatial and temporal changes in biological pumps (Kim et al., 2017b; Kim et al., 2020). Stable carbon and nitrogen isotopes (Nakanishi and Minagawa, 2003; Kwak et al., 2017), radiocarbon isotopes (Kim et al., 2020), and lipid biomarkers (Park et al., 2019b; Gal et al., 2021) have been examined in sinking particle samples to further understand the sources of organic matter.

Sinking particles exported from the euphotic layer contain mostly dead cells of phytoplankton and fecal pellets of zooplankton. These components are utilized by detritivores and bacteria (Busch et al., 2017; Gloeckler et al., 2018; Van Der Jagt et al., 2020). The organic matter composition of sinking particles is altered by microbial degradation during vertical transit (Gupta and Kawahata, 2000). One way to assess the degradation of sinking organic matter is to examine the composition of amino acids (AAs), which represent labile compounds in aquatic environments (Lee and Cronin, 1984). The relative composition of AAs has been used as a diagenetic indicator of the magnitude of microbial alteration of organic matter (Dauwe et al., 1999; Ingalls et al., 2003; Nagel et al., 2016). Recently, compound-specific isotope analysis of AAs (CSIA-AAs) has been used to understand trophic dynamics in marine ecology (McMahon and McCarthy, 2016; Ohkouchi et al., 2017). Nitrogen isotope ratios of individual AAs ( $\delta^{15}\text{N}_{\text{AA}}$ ) has helped differentiate between trophic transfer and nitrogen baseline of consumers in the food web as trophic and source AAs, respectively (Chikaraishi et al., 2009; Bowes and Thorp, 2015). The difference between trophic and source AAs could be expressed as the trophic position (TP) of an organism regardless of the nitrogen baseline fluctuation (Chikaraishi et al., 2014). For non-living organic matter, TP values can be used to assess the relative contributions of organic matter derived from autotrophic and heterotrophic organisms (Batista et al., 2014). The wide distribution of TP values in sinking particles indicates various ratios of autotrophs and heterotrophs in exported particles from euphotic layers (Shen et al., 2021).

The objective of this study was to examine the seasonal variation in the trophic structure of the planktonic ecosystem in the UB using the nitrogen isotope ratio of the AAs of sinking

particles. In addition, diagenetic indicators were estimated using AA composition and  $\delta^{15}\text{N}_{\text{AA}}$  to assess the magnitude of microbial degradation in sinking particles.

## MATERIALS AND METHODS

### Sample Collection

Sinking particle samples were collected using time-series sediment traps (SMD26S-6000, Nichiyu Giken Kogyo Co. Ltd., Kawagoe, Japan) with a sampling interval of 14 days at depths of 1000 and 2250 m in the Ulleung Basin (37°21' N, 131°23' E; 2323 m water depth, **Figure 1**). Sample handling and splitting have been described previously (Kim et al., 2017b). The sinking particle samples were oven-dried and homogenized for further experiments. The 8-days interval Chlorophyll-a data of MODIS with 0.1 degrees resolution from 2017 to 2018 near the study site (37°35' N, 131°45' E) was obtained from the NASA Earth Observation website (<http://neo.gsfc.nasa.gov>). The 2-months interval water temperature and salinity near the study site (37°55' N, 131°24' E) from 2017 to 2018 were downloaded from the National Institute of Fisheries Science website ([nifs.go.kr](http://nifs.go.kr)). Nitrate concentration data during 2017 (for 2 months interval) near the study site (37°55' N, 131°24' E) was obtained from the National Institute of Fisheries Science website ([nifs.go.kr/kodc/soo\\_list.kodc](http://nifs.go.kr/kodc/soo_list.kodc)). The monthly Nitrate concentration data during 2018 near the study site (37°50' N, 131°50' E) was obtained from the World Ocean Atlas ([ncei.noaa.gov/products/world-ocean-atlas](http://ncei.noaa.gov/products/world-ocean-atlas)) (Garcia et al., 2019).

### Total Mass, Lithogenic, Particulate Organic Carbon Fluxes, and Al Contents

Total mass flux of the sinking particles was determined gravimetrically by weighing the samples dried at 45°C in an oven. For organic carbon content measurement, ~10 mg of each dried sample was weighed in a silver capsule and fumigated with concentrated HCl vapor in a desiccator at room temperature for 20 hours to remove inorganic carbon (Hedges and Stern, 1984; Komada et al., 2008; Kim et al., 2017b). Fumigated samples were placed on a hot plate at 45°C for 4 hours to remove the remaining acid and enclosed in tin capsules. Carbon content was measured using an elemental analyzer (2400 Series II, PerkinElmer, US) with the uncertainty of 0.2% RSD based on the duplicate sample analysis. Al content of the sinking particle samples was analyzed using inductively coupled plasma optical emission spectrometer (ICP-OES, Optima 8300, PerkinElmer, US) at the Korea Basic Science Institute (KBSI). For calibration, two standard materials (SRM 1646a, and SRM 2702, NIST, US) were analyzed. Lithogenic material content was estimated by multiplying the content of Al by a factor of 12.15 (Taylor and McLennan, 1985).

### Bulk Nitrogen Isotope Analysis

Total nitrogen contents and stable nitrogen isotope ratios were measured using elemental analyzer (Vario Select, Elementar, Germany) coupled with isotope ratio mass spectrometer (VisION, Elementar, Germany). Approximately 5–8 mg of powdered sinking particle samples were packed into tin

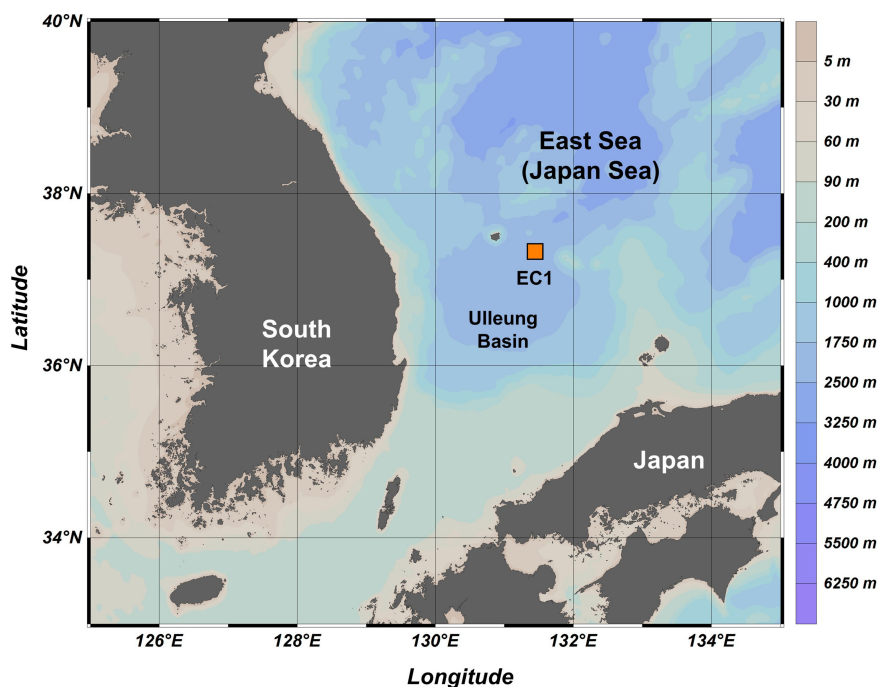


**FIGURE 1** | Sampling site of this study.

capsules. To check the precision of nitrogen isotope analysis, an international standard with certified  $\delta^{15}\text{N}$  values (IAEA N-1) was measured every 10 runs of samples. During sample analysis, analytical error of the standards was less than 0.3%.

## AA Derivatization, Quantification, and Nitrogen Isotope Ratio Analysis

Approximately 100–200 mg of dry samples was hydrolyzed (6 M HCl, 20 h, 110°C). The large particles were removed using syringe filter (0.45  $\mu\text{m}$  pore size) after cooling to room temperature. Lipids were removed using 6:5 n-hexane/dichloromethane (v/v). Residual HCl in the samples was removed by blowing  $\text{N}_2$  gas at 70°C. Purification was conducted using a cation exchange column (AG-50X W8, 200–400  $\mu\text{m}$  mesh, Bio-Rad), following Takano et al. (2010). AAs were eluted with 10%  $\text{NH}_4\text{OH}$  solution. Each sample was dried with  $\text{N}_2$  gas and dissolved in methanol. AAs in the samples were derivatized with 1:4 thionyl chloride/isopropanol (v/v) and 1:4 pivaloyl chloride/dichloromethane (v/v). AA derivatives were extracted using 6:5 n-hexane/dichloromethane (v/v).

AAs were identified from the mass spectra and retention times of standard mixtures of AA derivatives (alanine, glycine,  $\beta$ -alanine, valine, leucine, isoleucine, norleucine,  $\gamma$ -aminobutyric acid, proline, aspartic acid, threonine, serine, methionine, glutamic acid, phenylalanine, and lysine) using gas chromatography coupled with mass spectrometry (GC/MS, Shimadzu GC 2010, Japan). AA concentrations were analyzed using a gas chromatograph equipped with a flame ionization detector (GC/FID, Shimadzu GC 2010, Japan). An HP-ultra2

column (25 m length, 0.32 mm inner diameter, and 0.52  $\mu\text{m}$  film thickness) was used for both GC/MS and GC/FID instruments. Helium was used as the carrier gas with a constant flow of 1.2 ml/min. The initial oven temperature was 40°C, which was increased at a rate of 15°C/min to 110°C, 3°C/min to 150°C, 6°C/min to 220°C (10 min), and finally 20°C/min to 250°C (8 min). We used the calibration curve of AA derivatives of the standard mixture to calculate AA concentrations. Calibration standards of 100%, 50%, 25%, 10%, 5%, and 2.5% were used, based on 3125  $\mu\text{M}$  AA homologues ( $R^2 > 0.995$  for all AAs).

The nitrogen isotope ratios of the individual AAs were measured using a gas chromatograph (HP 6890N, Agilent Technologies, US) connected to a furnace (GC5 Interface, Elementar, Germany) and an isotope ratio mass spectrometer (Isoprime 100, Elementar, Germany). An HP-ultra2 column (50 m length, 0.32 mm inner diameter, and 0.52  $\mu\text{m}$  film thickness) was used. Helium was used as the carrier gas with a constant flow of 1.5 ml/min. We used the same oven program for GC/MS and GC/FID analysis. A standard mixture of AA derivatives (alanine, glycine, valine, leucine, norleucine, proline, aspartic acid, methionine, glutamic acid, and phenylalanine) with certified  $\delta^{15}\text{N}$  values were measured every five runs of samples to check instrumental precision and to calibrate raw  $\delta^{15}\text{N}$  values with drift correction ( $R^2 > 0.995$  between known and measured  $\delta^{15}\text{N}$  values). Samples were injected 2–3 times for the replicate analysis. Some AAs, including aspartic acid and threonine, were excluded because of poor peak separation and isotopic reproducibility in the isotope analysis. The standard deviations of the  $\delta^{15}\text{N}$  values of the AA standards were lower than 1%.

## Data Processing

The Pearson correlation coefficients were determined by using the data of sinking fluxes (total mass, lithogenic, POC, TN, and THAA) and  $\delta^{15}\text{N}$  values (bulk and THAA).

The degradation index (DI) was calculated using relative molar abundance of AAs using the following equation (Dauwe et al., 1999).

$$DI = \sum \left( \frac{(var_i - AVG_i)}{STD_i} * factor\ coefficient_i \right)$$

where  $var_i$  is molar % of AA<sub>*i*</sub>. We used  $AVG_i$ ,  $STD_i$ , and factor coefficient<sub>*i*</sub> from the reference dataset, including average, standard deviation, and first axis of factor coefficient of AA<sub>*i*</sub> from a previous study (Dauwe et al., 1999).

The  $\delta^{15}\text{N}$  value of THAA ( $\delta^{15}\text{N}_{THAA}$ ) was calculated by molar %-weighted average of individual  $\delta^{15}\text{N}_{AA}$  with following equation (McCarthy et al., 2013).

$$\delta^{15}\text{N}_{THAA} = \sum (\delta^{15}\text{N}_{AA} * mol\ \% \text{ of AA})$$

Where  $\delta^{15}\text{N}_{AA}$  is the individual  $\delta^{15}\text{N}$  value of AAs measured in this study (Ala, Gly, Val, Leu, Ile, Pro, Glu, Phe). The mol % of AA is the molar percentage of AA quantified using GC/FID.

TP was calculated using the following equation (Chikaraishi et al., 2009).

$$TP = \left( \frac{\delta^{15}\text{N}_{Glu} - \delta^{15}\text{N}_{Phe} - \beta}{TDF} \right) + 1$$

where  $\delta^{15}\text{N}_{Glu}$  is average nitrogen isotope ratio of glutamic acid and  $\delta^{15}\text{N}_{Phe}$  is the nitrogen isotope ratio of phenylalanine. The  $\beta$  value is the difference in  $\delta^{15}\text{N}$  between glutamic acid and phenylalanine in primary producers. TDF is the trophic enrichment factor of  $\delta^{15}\text{N}_{Glu}$  relative to  $\delta^{15}\text{N}_{Phe}$  in a trophic transfer. In this study, 3.4‰ and 7.6‰ were used as the  $\beta$  and TDF values, respectively (Chikaraishi et al., 2009). The propagation of error in TP estimation was calculated by the equation in Ohkouchi et al. (2017).

$\Sigma V$  value was calculated by the isotopic variance of trophic AAs, using the following equation (McCarthy et al., 2007).

$$\Sigma V = \sum \left( \frac{|\delta^{15}\text{N}_{AA} - \delta^{15}\text{N}_{Trophic\ AA}|}{n} \right)$$

Where  $\delta^{15}\text{N}_{AA}$  is the value of each trophic AA and  $\delta^{15}\text{N}_{Trophic\ AA}$  is the average nitrogen isotope ratio of the six trophic AAs (Ala, Val, Leu, Ile, Pro, and Glu).  $n$  is the number of trophic AAs used in the equation.

## RESULTS

The seasonal variations of water temperature and salinity were displayed in **Figures 2A, B**, respectively. In June 2017 and 2018, relatively warm (> 20°C) and salty (> 34.5 psu) water mass (High Salinity Tsushima Warm Water) was introduced in the study site. From August to October, that water mass was placed below

the low salinity surface water, generating a strong halocline. Surface water from late summer to early autumn showed relatively lower salinity (< 34 psu) and was known as Low Salinity Tsushima Warm Water, which originated from Changjiang river discharge water (Park et al., 2016b). In December, upper 100 m of water column was almost homogenized in both years. Nitrate was mostly depleted in surface water except during winter (**Figure 2C**). In January 2018, greater concentration of nitrate (> 30  $\mu\text{M}$ ) was observed in 100 m water depth. MODIS-observed surface Chlorophyll-a concentration was the highest (3.5  $\mu\text{g}/\text{m}^3$ ) in April 2017 (**Figure 2D**). Double peaks of surface Chl-a concentrations in March (1.7  $\text{mg}/\text{m}^3$ ) and April (1.9  $\text{mg}/\text{m}^3$ ) were observed in 2018.

The total mass fluxes ranged between 118–339  $\text{mg m}^{-2} \text{d}^{-1}$  at 1000 m and 150–494  $\text{mg m}^{-2} \text{d}^{-1}$  at 2250 m (**Figure 3A** and **Table S1, S2**). Clear monthly variations were observed in the total mass fluxes at both depths. The total mass flux at 2250 m gradually increased and was larger than that at 1000 m from October 2017. Lithogenic fluxes ranged 14.3–85.1  $\text{mg m}^{-2} \text{d}^{-1}$  at 1000 m and 45.7–144.2  $\text{mg m}^{-2} \text{d}^{-1}$  at 2250 m (**Figure 3A** and **Table S1**). The seasonal variations of lithogenic fluxes were similar to those of total mass fluxes, showing significant correlation at 2250 m ( $R^2 = 0.88$ ,  $p = 0.000$ ), rather than at 1000 m ( $R^2 = 0.54$ ,  $p = 0.027$ ). The POC fluxes were 5.9–28.3  $\text{mg m}^{-2} \text{d}^{-1}$  at 1000 m and 10.3–26.6  $\text{mg m}^{-2} \text{d}^{-1}$  at 2250 m. The POC flux at 1000 m was the largest in October and gradually decreased until March 2018. However, at 2250 m, the POC flux was the largest in February and relatively constant from autumn to winter. The contribution of POC to total mass flux ranged between  $8.3 \pm 2.5\%$  at 1000 m and  $6.2 \pm 1.0\%$  at 2250 m (**Figure 3B**). The POC percentage was mostly greater at 1000 m than at 2250 m. The POC percentage in sinking particles was highest in August and declined from autumn. However, at 2250 m, the decrease in the percentage of POC in sinking particles was relatively weak since autumn.

Total nitrogen (TN) fluxes (**Figure 4**) were highly correlated with total mass fluxes at 1000 m ( $R^2 = 0.51$ ,  $p = 0.036$ ) and 2250 m ( $R^2 = 0.80$ ,  $p = 0.000$ ). The TN values at 1000 m were maximum from October to November 2017 and gradually decreased during winter. On the other hand, TN values at 2250 m increased during the entire study periods and were highest in February 2018. Total hydrolysable AA (THAA) fluxes were 0.5–4.1  $\text{mg m}^{-2} \text{d}^{-1}$  at 1000 m and 1.0–6.0  $\text{mg m}^{-2} \text{d}^{-1}$  at 2250 m (Table S1 and S2), accounting for 3.5%–10.8% and 3.8%–13.4% of POC fluxes at 1000 and 2250 m, respectively. THAA fluxes showed a relatively weak correlation with total mass ( $R^2 = 0.34$ ,  $p = 0.185$ ) as compared to POC fluxes ( $R^2 = 0.75$ ,  $p = 0.001$ ) at 1000 m. In contrast, THAA fluxes at 2250 m showed a more significant correlation with both total mass ( $R^2 = 0.56$ ,  $p = 0.019$ ) and POC ( $R^2 = 0.51$ ,  $p = 0.035$ ) fluxes. The THAA fluxes at 1000 m were mostly larger than those at 2250 m from August to November 2017, whereas during winter, THAA fluxes at 2250 m were twice than those at 1000 m. The THAA-N/TN percentages at 2250 m were mostly greater than those at 1000 m, implying THAA-N supply is not solely derived from sinking flux (**Figure 4**).

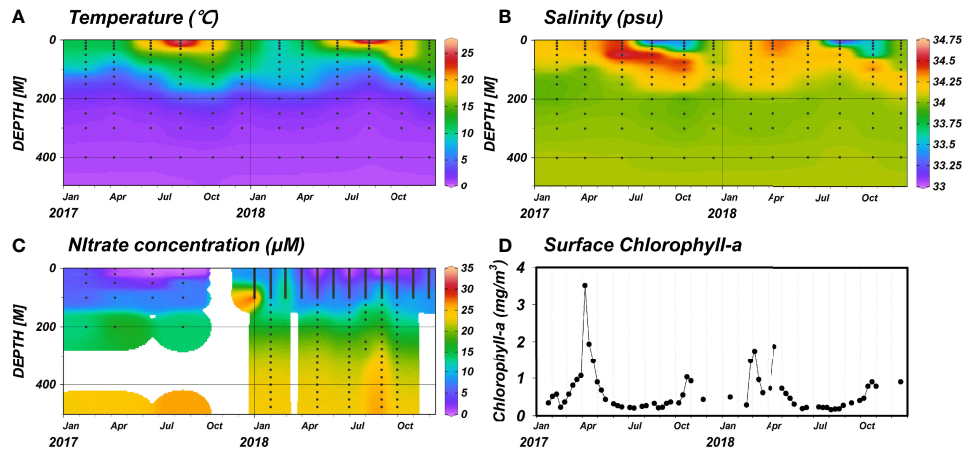


**FIGURE 2** | Water temperature (A), salinity (B), nitrate concentration (C), and surface chlorophyll-a concentration (D) near the study site.

The AA compositions varied between 1000 and 2250 m (Figure 5 and Tables S3, S4). Among the AAs, the molar percentages of two non-proteinaceous AAs ( $\beta$ -alanine (BALA) and  $\gamma$ -aminobutyric acid (GABA)) were significantly higher at 2250 m (4.3–7.1%) than at 1000 m (1.4–3.9%) (Figure 7A). At 1000 m, the molar percentages of BALA and GABA gradually increased over time and were the largest (3.9%) in February. However, they did not show any seasonal variation at 2250 m. The DI values were mostly higher at 1000 m than at 2250 m (Figure 7C). The DI values ranged from 0.6 to 1.8 at 1000 m and from  $-0.8$  to 0.3 at 2250 m. The DI values were relatively high in

November and March at 1000 m. Highest DI value at 2250 m was observed in November.

Bulk  $\delta^{15}\text{N}$  values of sinking particles (Figures 6A, B) displayed wide range from  $-3.4$ – $5.6$ ‰ at 1000 m and from  $-1.7$ – $3.9$ ‰ at 2250 m. Sinking particles at both depths showed apparent  $\delta^{15}\text{N}$  values decrease from January to March. Those seasonal patterns of bulk  $\delta^{15}\text{N}$  values showed clear correlation with THAA  $\delta^{15}\text{N}$  values at 1000 m ( $R^2 = 0.75$ ,  $p = 0.001$ ), but not with those at 2250 m ( $R^2 = 0.25$ ,  $p = 0.368$ ). We grouped the nitrogen isotope ratios of individual AAs into two categories: trophic AAs (Ala, Val, Leu, Ile, Pro, and Glu) and source AAs

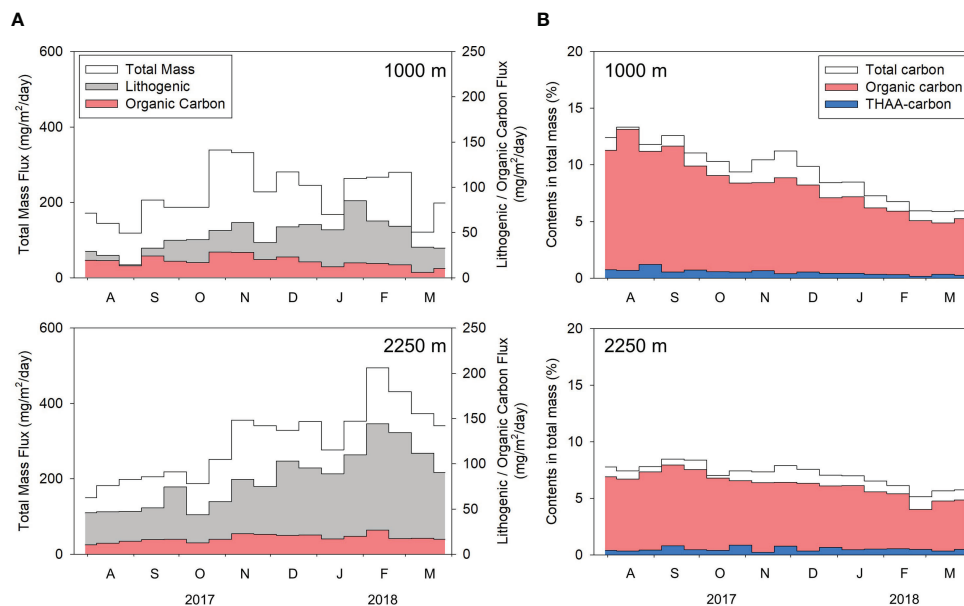
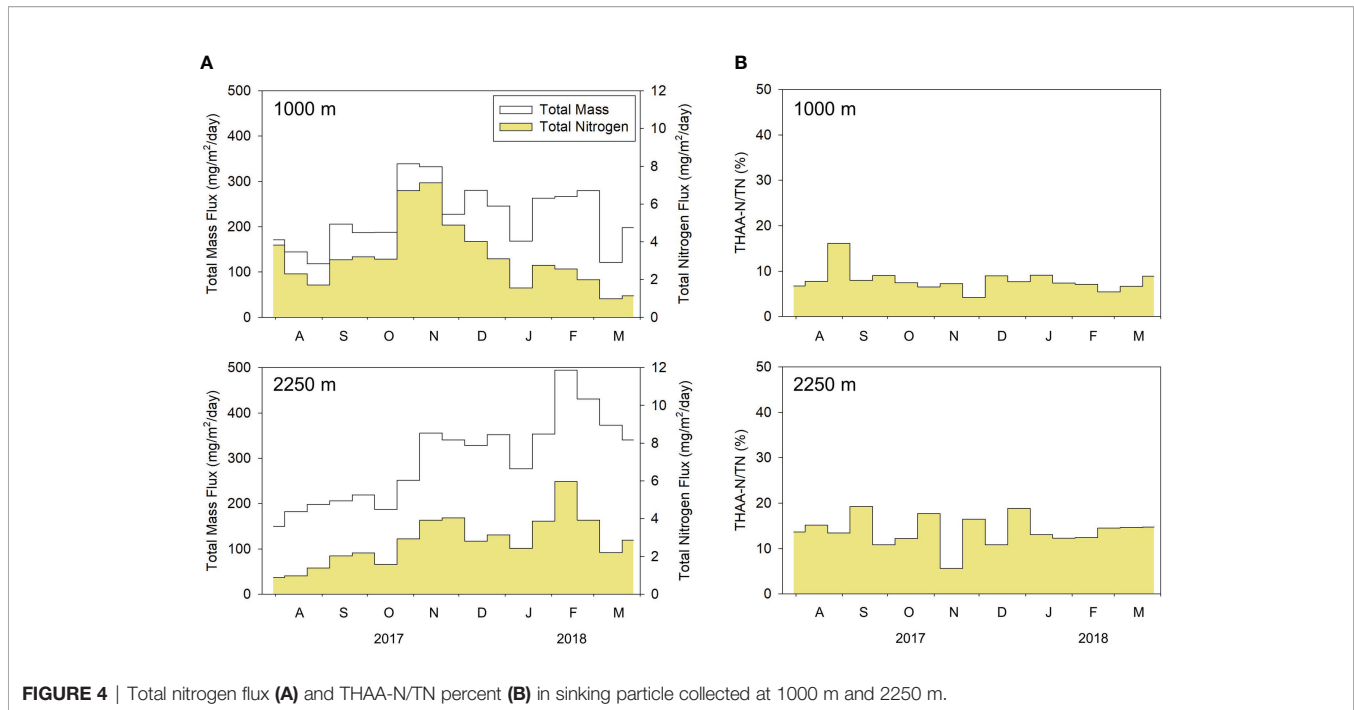


**FIGURE 3** | Total mass flux, lithogenic flux, organic carbon flux (A), and percentages of total, organic, and THAA carbon (B) for sinking particle collected at depths of 1000 m and 2250 m.



(Gly and Phe) (Figures 6C, D and Tables S5, S6). Trophic AAs showed a wide  $\delta^{15}\text{N}$  range at both depths (0.4–19.7‰ at 1000 m and 0.3–16.0‰ at 2250 m), whereas the source AAs showed a narrow  $\delta^{15}\text{N}$  range (–1.9–3.8‰ at 1000 m and –1.8–5.4‰ at 2250 m). The  $\delta^{15}\text{N}$  values of both trophic and source AAs were the highest in October and largely decreased from November 2017 to the end of the study period. Among trophic AAs, the  $\delta^{15}\text{N}$  values of Ala, Leu, and Ile decreased by ~10‰ from October to March at both depths.

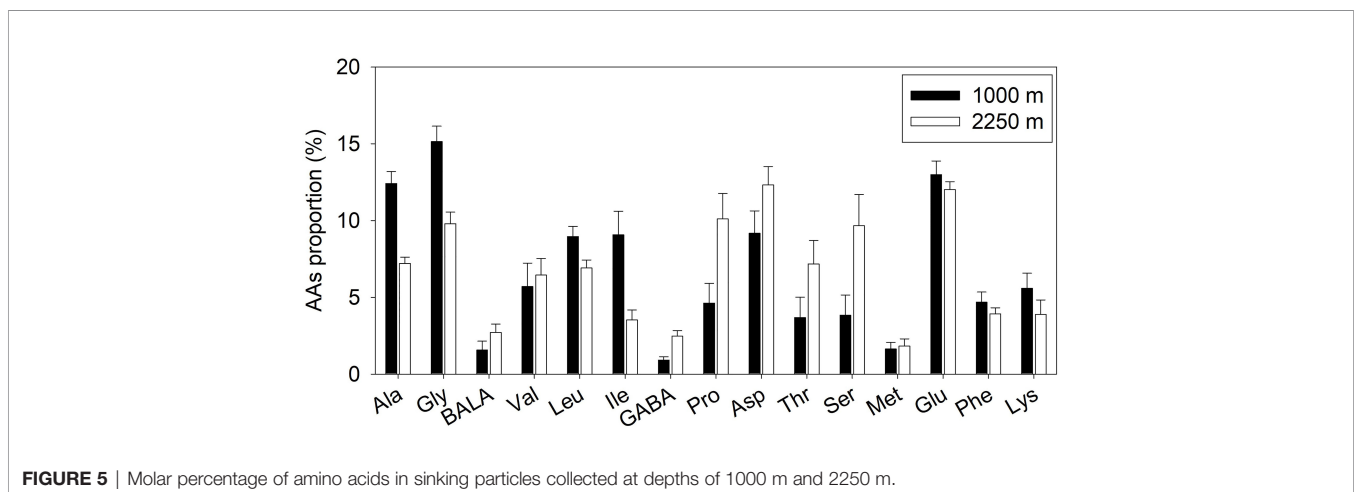
The  $\Sigma\text{V}$  values (Figure 7B and Tables S5, S6) were mostly lower at 1000 m (0.7–2.9) than those at 2250 m (1.7–3.5). Sinking particles at 1000 m showed a larger increase in  $\Sigma\text{V}$  values (1.9) as compared to those at 2250 m (0.9) from July 2017 to March 2018. TP was usually higher at 1000 m (1.5–3.1) than at 2250 m (1.3–

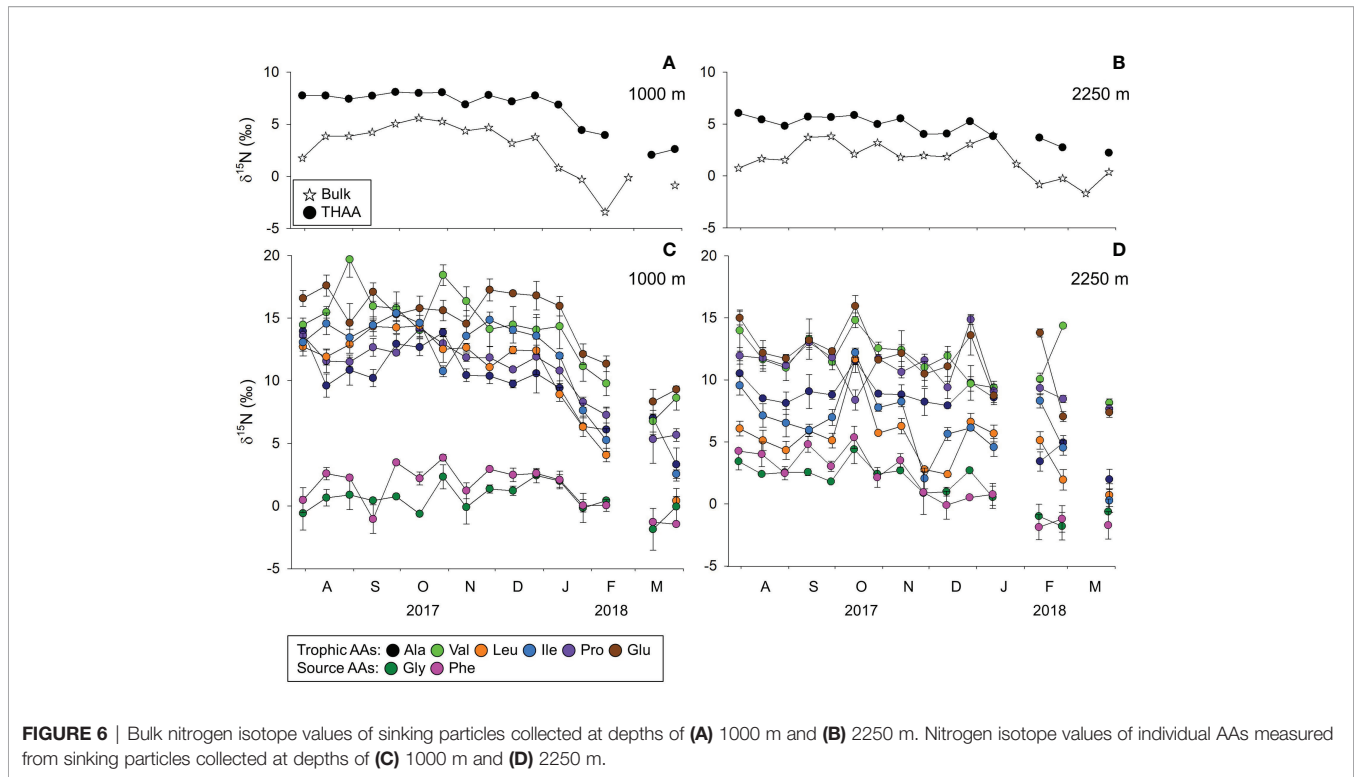
2.2), with the exception of February 2018 (Figure 7D and Tables S4, S5). The TP values at 1000 m gradually decreased (2.9 to 2.0) from September 2017 to March 2018, whereas the TP values at 2250 m increased (1.7 to 2.6) from November 2017 to February 2018.

## DISCUSSION

### Particle Fluxes and Compositions Between 1000 and 2250 m Water Depths

A previous study in the UB, conducted from 2011 to 2012 (Kim et al., 2017b), showed that POC fluxes between 1000 and 2300 m were mostly similar, and lithogenic fluxes were apparently larger

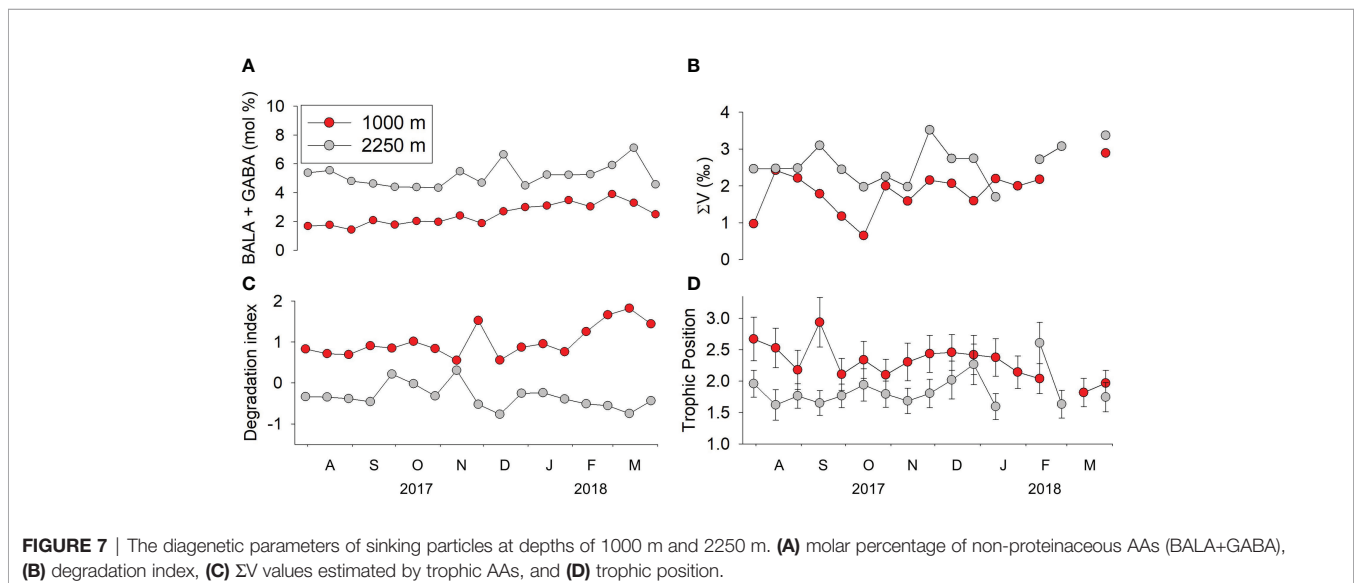




at 2300 m than at 1000 m. Additionally, Kim et al. (2020) reported that the warm core eddy during El Niño (2015–2016) enhanced organic carbon and lithogenic fluxes of sinking particles and potentially invoked sediment mobilization and transport from the Korea Strait and/or shelf and slope of the UB region. These results imply that the mesopelagic and bathypelagic layers in the UB are not solely influenced by the sinking flux from the euphotic layer. Thus, assessing the organic matter composition of sinking particles would provide important

information for understanding the seasonal and interannual variation of downward organic particle sources.

In 2017, the strong halocline in August persisted until October, and active vertical mixing was found in December (Figure 2B). The upward supply of nutrients within 100 m water depth was observed from January 2018, likely fuelling phytoplankton bloom from late February (Figure 2C). Those annual variations of nitrate (Figure 2C) and Chlorophyll-a (Figure 2D) showed similar pattern to previous studies, suggesting the pelagic production



regulate seasonal variation of sinking particle fluxes (Kwak et al., 2013; Joo et al., 2014; Rho et al., 2016).

The AA concentrations of sinking particle and sediment decrease rapidly through microbial degradation in marine environment, and the relative proportions of AAs are altered by microbial activity (Dauwe et al., 1999). THAA fluxes in sinking particles are usually correlated with the total mass and organic carbon fluxes (Gupta and Kawahata, 2000; Honjo et al., 2000; Ingalls et al., 2006). In this study, THAA fluxes at 1000 m were significantly correlated with organic carbon flux, but not with total mass flux. The POC contributions to total mass fluxes were mostly smaller at 2250 m than at 1000 m (**Figure 3B**). Interestingly, the POC percentage and total mass flux displayed seasonally different trends. The total mass flux at 1000 m was the largest between October and November, but gradually decreased from November. The total mass flux at 2250 m was the highest in February. However, both water depths showed a continuous decline in the POC percentage from summer to the next spring. This trend is apparently different from the seasonal POC fluxes at both water depths, indicating that the contributions of lithogenic fluxes to total mass fluxes increased from the summer of 2017 to early spring of 2018 (**Figure 3A**). Kim et al. (2017b) suggested that aeolian lithogenic and organic particles could be important components of sinking particles at 1000 m in the UB, using Al contents and radiocarbon isotopes. In addition, lithogenic fluxes at 1000 and 2000 m in the UB are supported by the supply of clay minerals by lateral transport and resuspension from the seafloor, as demonstrated using excess Mn contents and radiocarbon isotopes (Kim et al., 2020). Thus, sinking particles at both 1000 and 2000 m in the UB should contain different proportions of downward particles and additional supply from resuspension and lateral transport. This result suggests that sinking particles would show different organic matter contents and their degree of microbial degradation between 1000 m and 2250 m water depths.

## Seasonal Variation of Basal Nitrogen Sources in the East Sea

The application of CSIA-AA is based on the separation of trophic enrichment and baseline  $\delta^{15}\text{N}$  in consumers, characterizing trophic and source AAs, respectively. Thus, both trophic and source AAs have been widely used to understand marine ecology and biogeochemistry (Sherwood et al., 2014; Pomerleau et al., 2017; Shen et al., 2021). The  $\delta^{15}\text{N}_{\text{THAA}}$  values were larger than bulk  $\delta^{15}\text{N}$  values, due to the dominant molar contribution of trophic AAs, which have greater  $\delta^{15}\text{N}$  values compared to bulk and source AAs. The  $\delta^{15}\text{N}_{\text{THAA}}$  values of sinking particles at 1000 m showed significant correlation with bulk  $\delta^{15}\text{N}$  values, although the contribution of THAA to TN percent was less than 20% (**Figure 4B**). In contrast, THAA-N/TN percent at 2250 m were relatively larger compared to those at 1000 m, and the correlation between  $\delta^{15}\text{N}_{\text{THAA}}$  and bulk  $\delta^{15}\text{N}$  values at 2250 m were not clear, suggesting different organic matter sources between two sampling depths as mentioned in previous section. Nevertheless, our data showed generally decreasing trends of the  $\delta^{15}\text{N}$  values of the bulk and AAs from

autumn to early spring. These results were previously observed by bulk  $\delta^{15}\text{N}$  values of sinking particles collected in the East Sea (Nakanishi and Minagawa, 2003; Kwak et al., 2017).

Phenylalanine  $\delta^{15}\text{N}$  ( $\delta^{15}\text{N}_{\text{Phe}}$ ) can trace the baseline  $\delta^{15}\text{N}$  in the food web (McClelland and Montoya, 2002; Popp et al., 2007). Microbial degradation of AAs occurs non-selectively (McCarthy et al., 2007) and usually increases the  $\delta^{15}\text{N}$  values of residual AAs in dissolved organic matter (Calleja et al., 2013; Yamaguchi and McCarthy, 2018). Microbial degradation can alter even  $\delta^{15}\text{N}_{\text{Phe}}$  values in detrital substrates by external hydrolysis of proteinaceous material (Hannides et al., 2013; Ohkouchi et al., 2017). However, the  $\delta^{15}\text{N}_{\text{Phe}}$  decreased by 5.3‰ at 1000 m and 3.9‰ at 2250 m from late October to March, suggesting a substantial decrease in  $\delta^{15}\text{N}$  baseline at both depths (**Figure 4**). Possible reasons for such a decrease might be the increase in atmospheric deposition of inorganic nitrogen fueling primary production (Kim et al., 2017a; Park et al., 2019a) and utilization of nitrogen sources in primary production (Nakanishi and Minagawa, 2003). In this study, the POC flux decreased gradually, and the microbial records increased during autumn and winter, as demonstrated by the diagenetic indicators. Atmospheric nitrogen derived from fertilizers and fossil fuels usually ranges between  $\delta^{15}\text{N}$  values of 0––2‰ (Kim et al., 2017a). Nitrate  $\delta^{15}\text{N}$  values in aerosols range from –17.2 to 6.5‰, as reported in the central part of Taiwan (Guha et al., 2017). Kim et al. (2017a) suggested that atmospheric nitrogen deposition from inland China influences the  $\delta^{15}\text{N}$  values of sediments in the Yellow Sea and East Sea. In winter, the atmospheric nitrogen (ammonia and nitrate) showed higher concentrations compared to other seasons (Park et al., 2019a), but their seasonal flux is usually low because of minimum precipitation (Yan and Kim, 2015). According to the models, approximately 10%–15% of annual new production, and up to 25% of summer/early autumn new production in the southern East Sea could be attributed to the atmospheric deposition of nitrogen (Onitsuka et al., 2009; Kang et al., 2010). Thus, this additional nitrogen input from the atmosphere could not significantly reduce the  $\delta^{15}\text{N}$  values of sinking particles from winter to early spring. Another possible cause of the  $\delta^{15}\text{N}_{\text{Phe}}$  decline could be an increase in dissolved inorganic nitrogen availability. Nakanishi and Minagawa (2003) suggested that enhanced nutrient availability by vertical mixing should cause relatively lighter nitrogen isotope assimilation through primary production in the euphotic layer, resulting in lower  $\delta^{15}\text{N}$  values of sinking particles in winter in the East Sea. In this study, water column was completely mixed within 100 m water depth in winter, and nitrate concentration in surface mixed layer was the largest in January 2018 (**Figure 2C**). Primary producers would assimilate more  $^{14}\text{N}$  of nitrate, resulting in declined  $\delta^{15}\text{N}$  values of both total nitrogen (Altabet et al., 1999) and AAs nitrogen (Shen et al., 2021) in sinking particles. A decrease in  $\delta^{15}\text{N}$  baseline was observed at both water depths (**Figures 6C, D**). In the East Sea, large amounts of organic particles in the euphotic layer can be rapidly transported by the active biological pump. This was also evidenced by the high organic carbon contents (2.6%–2.9%) in surface sediments (Lee et al., 2008).

## AA Compositions and Diagenetic Indicators

The THAA-N contents represent labile organic nitrogen within total nitrogen pool (Gupta and Kawahata, 2000). This study showed larger THAA-N/TN values in sinking particles at 2250 m than those at 1000 m (Figure 4B), suggesting additional AAs supplied by lateral transport and resuspension. Those different sources of organic nitrogen between 1000 m and 2250 m were also exhibited by AAs compositions (Figure 5). For example, glycine could be a potential indicator for microbial degradation (McCarthy et al., 2007; Calleja et al., 2013) because relative molar percent of glycine increase as microbial degradation proceeds, as selective preservation of glycine by siliceous exoskeletons of diatom cells (Hecky et al., 1973; Pantoja and Lee, 2003). However, our results showed molar percent of glycine at 1000 m ( $15.1 \pm 1.0\%$ ) were greater than those at 2250 m ( $9.8 \pm 0.8\%$ ), even though sinking particles at 2250 m were more microbially degraded as revealed by diagenetic indicators (Figures 7A–C). This suggests the source composition of AAs should be different especially for sinking particles at 2250 m, including additional sources of organic matter through lateral transport processes. Possible sources of sinking organic matter at 2250 m in the UB region could be derived from shelf and slope, displaying considerable organic carbon fluxes from lateral transport ( $4.5\text{--}7.8 \text{ g C m}^{-2} \text{ year}^{-1}$ ), compared to those from vertical flux ( $5.1\text{--}5.8 \text{ g C m}^{-2} \text{ year}^{-1}$ ) from the water column (Lee et al., 2019). This result explains the amounts of organic matter at 2250 m could be larger than those at 1000 m, and the detailed organic matter composition should be different between two sampling depths.

Non-proteinaceous AAs, BALA, and GABA can be used as diagenetic indicators and are the transformation products of microbial activity, with significant correlation with DI values (Dauwe et al., 1999; Vandewiele et al., 2009). They accounted for 2%–3% of the total AA concentration in sediment samples (Carstens and Schubert, 2012). The combined molar percentage of BALA and GABA was higher at 2250 m than at 1000 m (Figure 7A). Additionally, the DI showed significant differences at 1000 m and 2250 m (Figure 7C), along to changes in AA compositions through degradation processes, allowing evaluation of organic matter degradation (Dauwe and Middelburg, 1998). The ranges of DI values of sinking particles in this study were commonly observed in previous studies as well (Dittmar et al., 2001; Batista et al., 2014; Shen et al., 2021). In this study, the DI values at 2250 m were mostly negative and lower than those at 1000 m. These results indicate that organic particles at 2250 m experienced higher microbial degradation.

Temporally, the combined molar percentage of BALA and GABA at 1000 m gradually increased from September 2017 and was the highest in February 2018 (Figure 7A). The DI values at 1000 m were relatively high in December 2017 and February and March 2018 (Figure 7C). These results suggest that microbial degradation is significant during the less productive seasons, which showed low concentration of surface Chl-a (Figure 2D) and small export fluxes of organic carbon (Figure 3B) and total nitrogen (Figure 4B).

$\Sigma V$  values for algae and fresh organisms (1.0–1.5) differ from those of microbially degraded organic matter ( $> 1.5$ ), as reported in previous studies on non-selective and irregular microbial

degradation and resynthesis of AAs (McCarthy et al., 2007; Yamaguchi et al., 2017). Higher  $\Sigma V$  values at 2250 m than at 1000 m imply that organic matter at 2250 m underwent stronger microbial degradation and resynthesis. This is consistent with the implications gained from the BALA+GABA mol % and DI. Sinking particles at both water depths showed a gradual increase in  $\Sigma V$  values from August 2017 to March 2018 due to a decrease in organic carbon supply (Figure 3B), and the subsequently higher microbial signature in winter-early spring compared to late summer-autumn.

## Sources of Organic Matter in Sinking Particles Based on Trophic Position

The trophic position determined by the difference in  $\delta^{15}\text{N}$  between trophic and source AAs can exclude the temporal and/or spatial fluctuation of baseline  $\delta^{15}\text{N}$  at the bottom of the food web. The TP values of sinking particles are the average TP values of the aggregated organic components derived from the relevant living organisms as well as non-living organic matter such as fecal pellets, dead algae cells, and other organic debris (Batista et al., 2014). Primary producers usually display a TP of 1.0 (Chikaraishi et al., 2009). The TP values of sinking particles in the water column below the euphotic layer showed a wide range (1.3–1.9) (Figure 8). The average TP of the time-series sinking particle samples at 1000 m water depth in the East Sea was  $2.3 \pm 0.4$ , which is significantly greater than that observed at the same depth in the Equatorial Pacific Ocean (Figure 8). However, the TP values of sinking particles in the Equatorial Pacific Ocean were more enhanced at 3600 m than at 1000 m (McCarthy et al., 2007). Such results were caused by the largely preserved phytodetritus flux during 1992–1993, fueling deep-sea microbes and metazoans (Smith et al., 1996). Shen et al. (2021) reported that the enhanced carnivory of zooplankton increased the TP (up to 1.9) of sinking particles during the El Niño period (2002–2003) in Monterey Bay. In contrast, the phytoplankton community shifted to larger cells, shortening the food chain, and decreasing the TP of sinking particles in Monterey Bay during the other periods (Shen et al., 2021). In addition, Batista et al. (2014) suggested that a decrease in zooplankton biomass and an increase in Chl-a in the Santa Barbara Basin could have led to a decline in the TP values of sinking particles and sediment. Overall, the variation in TP values of sinking particles was likely controlled by the relative contribution of organic matter derived from phytoplankton and/or zooplankton (herbivorous, omnivorous, and carnivorous) biomass in the entire water column.

The average value ( $2.3 \pm 0.3$ ) of TP in the East Sea was much higher than those in other seas (Fig. 8), demonstrating larger contribution of relatively higher trophic position consumer-derived organic matter in the water column. For example, genus *Calanus*, one of the most dominant calanoid copepod in the East Sea, displayed 0.5 unit larger TP values ( $\sim 2.9$ ) compared those in other seas in the Korean peninsula (Kim et al., personal communication). It seems to be related with different trophic dynamics of planktonic food web structure, resulting from larger proportion of small (nano and pico) size phytoplankton to primary production in the East Sea (Joo et al., 2017; Jang et al., 2021). In addition, aerobic microbes may influence the enhanced TP values of sinking particles, but the effect of microbes attached

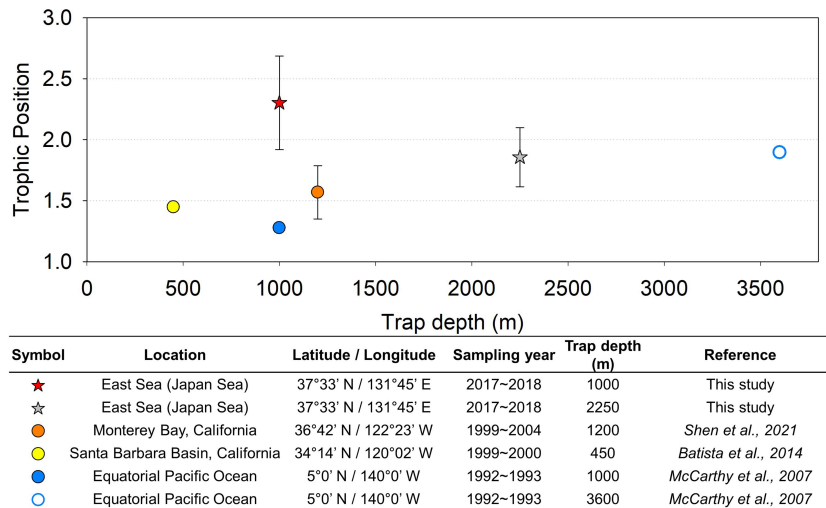


**FIGURE 8** | Trophic position of sinking particles in this study and reference literatures. Note that all TP values were calculated with same equation used in this study.

to the surface of sinking particles might be limited, considering much smaller abundance of microbial biomass and more positive DI values in the East Sea. Thus, the TP values of sinking particles in the East Sea suggest a predominantly zooplankton-derived organic matter, such as fecal pellets. Eglite et al. (2018) reported that the TP values of mesozooplankton (100–300  $\mu\text{m}$ ) were close to 3.0 in the central Baltic Sea, proposing that diazotrophic cyanobacteria or dinoflagellate as primary producers would be transferred to mesozooplankton *via* mixo- and/or heterotrophs. TP values of fecal pellets ranged 2.1 to 2.6 in a zooplankton mixture from Sargasso Sea and euphausiid in the Northeast Pacific, and were similar to those of the zooplankton body themselves (2.2–2.6) (Doherty et al., 2021). The higher TP values observed in this study could be related to the fecal pellet TP in the East Sea, which could be tightly coupled with omnivore and/or carnivore production, particularly at a water depth of 1000 m.

TP values varied in large ranges (1.3–3.1) seasonally and with depth. At 1000 m, the TP values of sinking particles were mostly over 2.0 (Figure 7D), suggesting that fecal pellets and other organic debris derived from heterotrophs were the dominant sources of sinking organic matter. Previous studies in the East Sea reported that the contribution of picoplankton (< 2  $\mu\text{m}$ ) to total primary production was up to 35% in summer (Joo et al., 2017). This picosized phytoplankton dominance would enhance the magnitude of the microbial loop in the euphotic layer, and the organic matter derived from higher trophic organisms could be occupied by sinking organic particles in nearly all seasons. On the other hand, zooplankton biomass in the East Sea is usually maximum in spring and minimum in winter in the upper layer of the water column (Iguchi, 2004; Park et al., 2016a). The seasonal variation in TP values of sinking particles reflects the average TPs of zooplankton communities and their biomass. The TP values of sinking particles at 1000 m were high (2.3–3.1) from July to September, and gradually decreased below 2.0 from late September to March. These seasonal variations of TP values were previously reported

in the Ulleung Basin, using ecological modeling and observational results of phytoplankton and zooplankton community composition and their biomass (Lee and Yoo, 2016). Thus, in winter, the decreased proportion of fecal pellets in sinking particles would result in the TP decline at 1000 m, probably due to the smaller biomass of zooplankton and decreased organic carbon flux. Rather, phytoplankton and its debris would contribute more to sinking particles and relative microbial activity would be enhanced, increasing  $\Sigma V$  values up to 2.9 in winter and early spring.

On the other hand, the TP values of sinking particles at 2250 m ( $1.9 \pm 0.2$ ) were mostly lower than those at 1000 m, indicating different sources of organic components between the two sampling depths. Possible sources of organic particles at 2250 m would be organic matter exported from 1000 m, resuspended from the seafloor, and advected from shelf and slope (Lee et al., 2019). Although the available literature is limited, previous studies have shown that the TP values of surface sediments (~1.0) can be lower than those of sinking particles (1.0–1.9) of sinking particles (Carstens et al., 2013; Batista et al., 2014). Previous study in the UB region reported the large amounts of excess Mn contents at 2300 m compared to those at 1000 m, suggesting high magnitude of sediment remobilization to the water column (Kim et al., 2017b). Such results would indicate sediment resuspension and lateral transport might be the causes for lower TP values of sinking particles at 2250 m in this study. In our study, TP values of sinking particles were usually lower at 2250 m than those at 1000 m for all seasons except February 2018, as in previous studies (Carstens et al., 2013; Batista et al., 2014). However, an increased TP value (2.6) was observed at 2250 m, with relatively larger organic carbon fluxes in February 2018 compared to those at 1000 m, suggesting a possibly larger contribution of organic particles derived from higher trophic organisms, caused by significant lateral transport in February 2018. Further study needs to elucidate the seasonal variation of input of lateral transport to UB region, for better understanding of organic matter dynamics in the East Sea.

The previous modeling study in the Ulleung Basin suggested the phytoplankton community will be shifted to smaller cells (flagellates and picophytoplankton) with cascading changes of planktonic food web structure in the future (Lee and Yoo, 2016). The decrease in primary production and the increase in small phytoplankton (< 2  $\mu\text{m}$ ) during recent decades has influenced the composition of the upper trophic level in the East Sea (Joo et al., 2014; Joo et al., 2017). In addition, particle size and residence time in the euphotic layer can affect the biological pump efficiency (Kwak et al., 2017). Our results suggest that the seasonal variation of TP values in sinking particles is controlled by relative biomass abundances of phytoplankton and zooplankton communities. The trophic position of sinking particles provides useful planktonic food web information to better understand the temporal and spatial changes of biological pumps in marine environments. Furthermore, the inter-annual variation of TP values in sinking particles would be helpful to understanding changes in the low trophic level food web structure in the East Sea according to the recently changing climate.

## CONCLUSION

In the present study, AAs concentrations and their nitrogen isotope ratios analysis of sinking particles in the East Sea were used to understand the relative contribution of organic matter derived from different trophic organisms, and how their relative proportions could differ according to season and depth. The nitrogen isotope ratio of phenylalanine of sinking particles, as used for nitrogen baseline, decreased during winter at both water depths (1000 m and 2250 m), suggesting a seasonal change in the dissolved inorganic nitrogen source for pelagic primary production. The TPs of sinking particles in the East Sea were apparently higher than those in other locations, probably due to more tightly coupled secondary production through zooplankton grazing. TP values demonstrated an apparent decreasing trend at 1000 m in winter and early spring, indicating a decline in the proportion of fecal pellets in sinking particles. In addition, sinking particles showed lower TP values at 2250 m than those at 1000 m in all seasons except for February 2018, probably due to the greater contribution of resuspended and/or laterally transported organic particles at 2250 m. On the other hand, the  $\Sigma\text{V}$  values of sinking particles at both depths indicated less planktonic organic matter fluxes and the following relatively more microbial alteration signature in winter and early spring, compared to those in late summer and autumn. Sinking particles at 2250 m reflected more significant microbial degradation than those at 1000 m, but the THAA-N/TN values

## REFERENCES

- Altabet, M. A., Pilskaln, C., Thunell, R., Pride, C., Sigman, D., Chavez, F., et al. (1999). The Nitrogen Isotope Biogeochemistry of Sinking Particles From the Margin of the Eastern North Pacific. *Deep. Sea. Res. Part I: Oceanograph. Res. Papers* 46, 655–679. doi: 10.1016/S0967-0637(98)00084-3
- Batista, F. C., Ravelo, A. C., Crusius, J., Casso, M. A., and McCarthy, M. D. (2014). Compound Specific Amino Acid  $\delta^{15}\text{N}$  in Marine Sediments: A New

were higher than those at 1000 m, with additional particle sources from resuspension and lateral transport. In this study, the TP and  $\Sigma\text{V}$  values in sinking particles revealed the relative proportions of organic matter derived from lower trophic level organisms, providing a better understanding of the seasonal variation of planktonic ecosystem structure in the water column.

## DATA AVAILABILITY STATEMENT

The original contributions presented in the study are included in the article/**Supplementary Material**. Further inquiries can be directed to the corresponding author.

## AUTHOR CONTRIBUTIONS

JH and GK provided sinking particle samples for analysis. YR operated trap sampler and estimated total mass, carbon, nitrogen, and lithogenic flux of sinking particles. HC conducted laboratory experiments and amino acid and isotope analyses. K-HS designed the experiments and revised the manuscript. All authors contributed to the article and approved the submitted version.

## FUNDING

This research was a part of the project titled ‘Deep Water Circulation and Material Cycling in the East Sea (20160400),’ funded by the Ministry of Oceans and Fisheries, Korea. This work was supported by the National Research Foundation of Korea (NRF) grants funded by the Ministry of Science and ICT (MSIT) (2021M3I6A1091270).

## ACKNOWLEDGMENTS

We appreciate the contributions of the members for their fieldwork during R/V Onnuri cruises.

## SUPPLEMENTARY MATERIAL

The Supplementary Material for this article can be found online at: <https://www.frontiersin.org/articles/10.3389/fmars.2022.824479/full#supplementary-material>.

Approach for Studies of the Marine Nitrogen Cycle. *Geochim. Cosmochim. Acta* 142, 553–569. doi: 10.1016/j.gca.2014.08.002

Bowes, R. E., and Thorp, J. H. (2015). Consequences of Employing Amino Acid vs. Bulk-Tissue, Stable Isotope Analysis: A Laboratory Trophic Position Experiment. *Ecosphere* 6, 1–12. doi: 10.1890/ES14-00423.1

Busch, K., Endres, S., Iversen, M. H., Michels, J., Nöthig, E.-M., and Engel, A. (2017). Bacterial Colonization and Vertical Distribution of Marine Gel Particles (TEP and CSP) in the Arctic Fram Strait. *Front. Marine Sci.* 4, 166. doi: 10.3389/fmars.2017.00166

- Calleja, M. L., Batista, F., Peacock, M., Kudela, R., and McCarthy, M. J. M. C. (2013). Changes in Compound Specific  $\delta^{15}\text{N}$  Amino Acid Signatures and D/L Ratios in Marine Dissolved Organic Matter Induced by Heterotrophic Bacterial Reworking. *Marine Chem.* 149, 32–44. doi: 10.1016/j.marchem.2012.12.001
- Carstens, D., Lehmann, M. F., Hofstetter, T. B., and Schubert, C. J. (2013). Amino Acid Nitrogen Isotopic Composition Patterns in Lacustrine Sedimenting Matter. *Geochim. Cosmochim. Acta* 121, 328–338. doi: 10.1016/j.gca.2013.07.020
- Carstens, D., and Schubert, C. J. (2012). Amino Acid and Amino Sugar Transformation During Sedimentation in Lacustrine Systems. *Organic Geochem.* 50, 26–35. doi: 10.1016/j.orggeochem.2012.06.006
- Chikaraishi, Y., Ogawa, N. O., Kashiwama, Y., Takano, Y., Suga, H., Tomitani, A., et al. (2009). Determination of Aquatic Food-Web Structure Based on Compound-Specific Nitrogen Isotopic Composition of Amino Acids. *Limnol. Oceanograph.: Methods* 7, 740–750. doi: 10.4319/lom.2009.7.740
- Chikaraishi, Y., Steffan, S. A., Ogawa, N. O., Ishikawa, N. F., Sasaki, Y., Tsuchiya, M., et al. (2014). High-Resolution Food Webs Based on Nitrogen Isotopic Composition of Amino Acids. *Ecol. Evol.* 4, 2423–2449. doi: 10.1002/ece3.1103
- Choi, D. H., Noh, J. H., and Shim, J. (2013). Seasonal Changes in Picocyanobacterial Diversity as Revealed by Pyrosequencing in Temperate Waters of the East China Sea and the East Sea. *Aquat. Microb. Ecol.* 71, 75–90. doi: 10.3354/ame01669
- Dauwe, B., and Middelburg, J. J. (1998). Amino Acids and Hexosamines as Indicators of Organic Matter Degradation State in North Sea Sediments. *Limnol. Oceanograph.* 43, 782–798. doi: 10.4319/lo.1998.43.5.0782
- Dauwe, B., Middelburg, J. J., Herman, P. M., and Heip, C. H. (1999). Linking Diagenetic Alteration of Amino Acids and Bulk Organic Matter Reactivity. *Limnol. Oceanograph.* 44, 1809–1814. doi: 10.4319/lo.1999.44.7.1809
- Dittmar, T., Fitznar, H. P., and Kattner, G. (2001). Origin and Biogeochemical Cycling of Organic Nitrogen in the Eastern Arctic Ocean as Evident From D-And L-Amino Acids. *Geochim. Cosmochim. Acta* 65, 4103–4114. doi: 10.1016/S0016-7037(01)00688-3
- Doherty, S. C., Maas, A. E., Steinberg, D. K., Popp, B. N., and Close, H. G. (2021). Distinguishing Zooplankton Fecal Pellets as a Component of the Biological Pump Using Compound-Specific Isotope Analysis of Amino Acids. *Limnol. Oceanograph.* 66, 2827–2841. doi: 10.1002/lno.11793
- Eglite, E., Wodarg, D., Dutz, J., Wasmund, N., Nausch, G., Liskow, I., et al. (2018). Strategies of Amino Acid Supply in Mesozooplankton During Cyanobacteria Blooms: A Stable Nitrogen Isotope Approach. *Ecosphere* 9, e02135. doi: 10.1002/ecs2.2135
- Gal, J.-K., Kim, J.-H., Kim, S., Hwang, J., and Shin, K.-H. (2021). Assessment of the Nutrient Diol Index (NDI) as a Sea Surface Nutrient Proxy Using Sinking Particles in the East Sea. *Marine Chem.* 231, 103937. doi: 10.1016/j.marchem.2021.103937
- García, H., Boyer, T., Baranova, O., Locarnini, R., Mishonov, A., Grodsky, A., et al. (2019). *World Ocean Atlas 2018: Product Documentation*. Ed. A Mishonov. doi: 10.13140/RG.2.2.34758.01602
- Gloekler, K., Choy, C. A., Hannides, C. C., Close, H. G., Goetze, E., Popp, B. N., et al. (2018). Stable Isotope Analysis of Micronekton Around Hawaii Reveals Suspended Particles are an Important Nutritional Source in the Lower Mesopelagic and Upper Bathypelagic Zones. *Limnol. Oceanograph.* 63, 1168–1180. doi: 10.1002/lno.10762
- Guha, T., Lin, C., Bhattacharya, S., Mahajan, A., Ou-Yang, C.-F., Lan, Y.-P., et al. (2017). Isotopic Ratios of Nitrate in Aerosol Samples From Mt. Lulin, a High-Altitude Station in Central Taiwan. *Atmosph. Environ.* 154, 53–69. doi: 10.1016/j.atmosenv.2017.01.036
- Gupta, L. P., and Kawahata, H. (2000). Amino Acid and Hexosamine Composition and Flux of Sinking Particulate Matter in the Equatorial Pacific at 175° E Longitude. *Deep. Sea. Res. Part I: Oceanograph. Res. Papers* 47, 1937–1960. doi: 10.1016/S0967-0637(00)00009-1
- Hannides, C. C., Popp, B. N., Choy, C. A., and Drazen, J. C. (2013). Midwater Zooplankton and Suspended Particle Dynamics in the North Pacific Subtropical Gyre: A Stable Isotope Perspective. *Limnol. Oceanograph.* 58, 1931–1946. doi: 10.4319/lo.2013.58.6.1931
- Hecky, R., Mopper, K., Kilham, P., and Degens, E. (1973). The Amino Acid and Sugar Composition of Diatom Cell-Walls. *Marine Biol.* 19, 323–331. doi: 10.1007/BF00348902
- Hedges, J. I., and Stern, J. H. (1984). Carbon and Nitrogen Determinations of Carbonate-Containing Solids 1. *Limnol. Oceanograph.* 29, 657–663. doi: 10.4319/lo.1984.29.3.0657
- Honjo, S., Francois, R., Manganini, S., Dymond, J., and Collier, R. (2000). Particle Fluxes to the Interior of the Southern Ocean in the Western Pacific Sector Along 170° W. *Deep. Sea. Res. Part II: Top. Stud. Oceanograph.* 47, 3521–3548. doi: 10.1016/S0967-0645(00)00077-1
- Iguchi, N. (2004). Spatial/temporal Variations in Zooplankton Biomass and Ecological Characteristics of Major Species in the Southern Part of the Japan Sea: A Review. *Prog. Oceanograph.* 61, 213–225. doi: 10.1016/j.pcean.2004.06.007
- Ingalls, A. E., Lee, C., Wakeham, S. G., and Hedges, J. I. (2003). The Role of Biominerals in the Sinking Flux and Preservation of Amino Acids in the Southern Ocean Along 170° W. *Deep. Sea. Res. Part II: Top. Stud. Oceanograph.* 50, 713–738. doi: 10.1016/S0967-0645(02)00592-1
- Ingalls, A. E., Liu, Z., and Lee, C. (2006). Seasonal Trends in the Pigment and Amino Acid Compositions of Sinking Particles in Biogenic CaCO<sub>3</sub> and SiO<sub>2</sub> Dominated Regions of the Pacific Sector of the Southern Ocean Along 170° W. *Deep. Sea. Res. Part I: Oceanograph. Res. Papers* 53, 836–859. doi: 10.1016/j.dsr.2006.01.004
- Jang, H.-K., Youn, S.-H., Joo, H., Kim, Y., Kang, J.-J., Lee, D., et al. (2021). First Concurrent Measurement of Primary Production in the Yellow Sea, the South Sea of Korea, and the East/Japan Sea 2018. *J. Marine Sci. Eng.* 9, 1237. doi: 10.3390/jmse9111237
- Joo, H., Park, J. W., Son, S., Noh, J. H., Jeong, J. Y., Kwak, J. H., et al. (2014). Long-Term Annual Primary Production in the Ulleung Basin as a Biological Hot Spot in the East/Japan Sea. *J. Geophysics. Res.: Ocean.* 119, 3002–3011. doi: 10.1002/2014JC009862
- Joo, H., Son, S., Park, J.-W., Kang, J. J., Jeong, J.-Y., Kwon, J.-I., et al. (2017). Small Phytoplankton Contribution to the Total Primary Production in the Highly Productive Ulleung Basin in the East/Japan Sea. *Deep. Sea. Res. Part II: Top. Stud. Oceanograph.* 143, 54–61. doi: 10.1016/j.dsr2.2017.06.007
- Kang, J., Cho, B. C., and Lee, C.-B. (2010). Atmospheric Transport of Water-Soluble Ions (NO<sub>3</sub><sup>-</sup>, NH<sub>4</sub><sup>+</sup> and Nss-SO<sub>4</sub><sup>2-</sup>) to the Southern East Sea (Sea of Japan). *Sci. Total. Environ.* 408, 2369–2377. doi: 10.1016/j.scitotenv.2010.02.022
- Kim, M., Hwang, J., Rho, T., Lee, T., Kang, D.-J., Chang, K.-I., et al. (2017b). Biogeochemical Properties of Sinking Particles in the Southwestern Part of the East Sea (Japan Sea). *J. Marine Syst.* 167, 33–42. doi: 10.1016/j.jmarsys.2016.11.001
- Kim, M., Kim, Y.-I., Hwang, J., Choi, K. Y., Kim, C. J., Ryu, Y., et al. (2020). Influence of Sediment Resuspension on the Biological Pump of the Southwestern East Sea (Japan Sea). *Front. Earth Sci.* 8, 144. doi: 10.3389/feart.2020.00144
- Kim, H., Lee, K., Lim, D.-I., Nam, S.-I., Kim, T.-W., Yang, J.-Y. T., et al. (2017a). Widespread Anthropogenic Nitrogen in Northwestern Pacific Ocean Sediment. *Environ. Sci. Technol.* 51, 6044–6052. doi: 10.1021/acs.est.6b05316
- Komada, T., Anderson, M. R., and Dorfmeier, C. L. (2008). Carbonate Removal From Coastal Sediments for the Determination of Organic Carbon and its Isotopic Signatures,  $\delta^{13}\text{C}$  and  $\Delta 14\text{C}$ : Comparison of Fumigation and Direct Acidification by Hydrochloric Acid. *Limnol. Oceanograph.: Methods* 6, 254–262. doi: 10.4319/lom.2008.6.254
- Kwak, J. H., Han, E., Hwang, J., Kim, Y. I., Lee, C. I., and Kang, C.-K. (2017). Flux and Stable C and N Isotope Composition of Sinking Particles in the Ulleung Basin of the East/Japan Sea. *Deep. Sea. Res. Part II: Top. Stud. Oceanograph.* 143, 62–72. doi: 10.1016/j.dsr2.2017.03.014
- Kwak, J., Lee, S., Park, H., Choy, E., Jeong, H., Kim, K., et al. (2013). Monthly Measured Primary and New Productivities in the Ulleung Basin as a Biological "Hot Spot" in the East/Japan Sea. *Biogeosciences* 10, 4405–4417. doi: 10.5194/bg-10-4405-2013
- Lee, C., and Cronin, C. (1984). Particulate Amino Acids in the Sea: Effects of Primary Productivity and Biological Decomposition. *J. Marine Res.* 42, 1075–1097. doi: 10.1357/002224084788520710
- Lee, J. S., Han, J. H., An, S. U., Kim, S. H., Lim, D., Kim, D., et al. (2019). Sedimentary Organic Carbon Budget Across the Slope of the Basin in the Southwestern Ulleung (Tsushima) Basin of the East (Japan) Sea. *J. Geophysics Res.: Biogeosci.* 124, 2804–2822. doi: 10.1029/2019JG005138

- Lee, T., Hyun, J.-H., Mok, J. S., and Kim, D. (2008). Organic Carbon Accumulation and Sulfate Reduction Rates in Slope and Basin Sediments of the Ulleung Basin, East/Japan Sea. *Geo-Mar. Lett.* 28, 153–159. doi: 10.1007/s00367-007-0097-8
- Lee, S., and Yoo, S. (2016). Interannual Variability of the Phytoplankton Community by the Changes in Vertical Mixing and Atmospheric Deposition in the Ulleung Basin, East Sea: A Modelling Study. *Ecol. Model.* 322, 31–47. doi: 10.1016/j.ecolmodel.2015.11.012
- McCarthy, M. D., Benner, R., Lee, C., and Fogel, M. L. (2007). Amino Acid Nitrogen Isotopic Fractionation Patterns as Indicators of Heterotrophy in Plankton, Particulate, and Dissolved Organic Matter. *Geochim. Cosmochim. Acta* 71, 4727–4744. doi: 10.1016/j.gca.2007.06.061
- McCarthy, M. D., Lehman, J., and Kudela, R. (2013). Compound-Specific Amino Acid  $\delta^{15}\text{N}$  Patterns in Marine Algae: Tracer Potential for Cyanobacterial vs. Eukaryotic Organic Nitrogen Sources in the Ocean. *Geochim. Cosmochim. Acta* 103, 104–120. doi: 10.1016/j.gca.2012.10.037
- McClelland, J. W., and Montoya, J. P. (2002). Trophic Relationships and the Nitrogen Isotopic Composition of Amino Acids in Plankton. *Ecology* 83, 2173–2180. doi: 10.1890/0012-9658(2002)083[2173:TRATNI]2.0.CO;2
- McMahon, K. W., and McCarthy, M. D. (2016). Embracing Variability in Amino Acid  $\delta^{15}\text{N}$  Fractionation: Mechanisms, Implications, and Applications for Trophic Ecology. *Ecosphere* 7. doi: 10.1002/ecs2.1511
- Nagel, B., Gaye, B., Lahajnar, N., Struck, U., and Emeis, K.-C. (2016). Effects of Current Regimes and Oxygenation on Particulate Matter Preservation on the Namibian Shelf: Insights From Amino Acid Biogeochemistry. *Marine Chem.* 186, 121–132. doi: 10.1016/j.marchem.2016.09.001
- Nakanishi, T., and Minagawa, M. (2003). Stable Carbon and Nitrogen Isotopic Compositions of Sinking Particles in the Northeast Japan Sea. *Geochem. J.* 37, 261–275. doi: 10.2343/geochemj.37.261
- Ohkouchi, N., Chikaraishi, Y., Close, H. G., Fry, B., Larsen, T., Madigan, D. J., et al. (2017). Advances in the Application of Amino Acid Nitrogen Isotopic Analysis in Ecological and Biogeochemical Studies. *Organic. Geochem.* 113, 150–174. doi: 10.1016/j.orggeochem.2017.07.009
- Onitsuka, G., Uno, I., Yanagi, T., and Yoon, J.-H. (2009). Modeling the Effects of Atmospheric Nitrogen Input on Biological Production in the Japan Sea. *J. Oceanograph.* 65, 433–438. doi: 10.1007/s10872-009-0038-4
- Onodera, J., Watanabe, E., Harada, N., and Honda, M. (2015). Diatom Flux Reflects Water-Mass Conditions on the Southern Northwind Abyssal Plain, Arctic Ocean. *Biogeosciences* 12, 1373–1385. doi: 10.5194/bg-12-1373-2015
- Pantoja, S., and Lee, C. (2003). Amino Acid Remineralization and Organic Matter Lability in Chilean Coastal Sediments. *Organic. Geochem.* 34, 1047–1056. doi: 10.1016/S0146-6380(03)00085-8
- Park, Y.-H., Kim, H. J., Son, J. W., Yoo, C. M., and Khim, B.-K. (2019b). Biomarker-Based Seawater Temperatures of Winter Sinking Particles and Core-Top Sediment in the Ulleung Basin of the East Sea. *Ocean Sci. J.* 54, 487–495. doi: 10.1007/s12601-019-0017-7
- Park, G.-H., Lee, S.-E., Kim, Y.-I., Kim, D., Lee, K., Kang, J., et al. (2019a). Atmospheric Deposition of Anthropogenic Inorganic Nitrogen in Airborne Particles and Precipitation in the East Sea in the Northwestern Pacific Ocean. *Sci. Total. Environ.* 681, 400–412. doi: 10.1016/j.scitotenv.2019.05.135
- Park, J. J., Park, K.-A., Kim, Y.-G., and Yun, J.-Y. (2016b). “Water Masses and Their Long-Term Variability,” in *Oceanography of the East Sea (Japan Sea)* (Cham, Switzerland: Springer), 59–86.
- Park, C., Suh, H.-L., Kang, Y.-S., Ju, S.-J., and Yang, E.-J. (2016a). “Zooplankton,” in *Oceanography of the East Sea (Japan Sea)*. Eds. K.-I. Chang, C.-I. Zhang, C. Park, D.-J. Kang, S.-J. Ju, S.-H. Lee and M. Wimbush (Cham: Springer International Publishing), 297–326.
- Pomerleau, C., Heide-Jørgensen, M. P., Ferguson, S. H., Stern, H. L., Høyer, J. L., and Stern, G. A. (2017). Reconstructing Variability in West Greenland Ocean Biogeochemistry and Bowhead Whale (*Balaena mysticetus*) Food Web Structure Using Amino Acid Isotope Ratios. *Polar Biol.* 40, 2225–2238. doi: 10.1007/s00300-017-2136-x
- Popp, B. N., Graham, B. S., Olson, R. J., Hannides, C. C., Lott, M. J., López-Ibarra, G. A., et al. (2007). Insight Into the Trophic Ecology of Yellowfin Tuna, *Thunnus albacares*, From Compound-Specific Nitrogen Isotope Analysis of Proteinaceous Amino Acids. *Terrest. Ecol.* 1, 173–190. doi: 10.1016/S1936-7961(07)01012-3
- Rho, T., Lee, T., and An, S. (2016). “Dissolved Oxygen and Nutrients,” in *Oceanography of the East Sea (Japan Sea)* (Cham, Switzerland: Springer), 149–168.
- Shen, Y., Guilderson, T. P., Sherwood, O. A., Castro, C. G., Chavez, F. P., and McCarthy, M. D. (2021). Amino Acid  $\delta^{13}\text{C}$  and  $\delta^{15}\text{N}$  Patterns From Sediment Trap Time Series and Deep-Sea Corals: Implications for Biogeochemical and Ecological Reconstructions in Paleorarchives. *Geochim. Cosmochim. Acta* 297, 288–307. doi: 10.1016/j.gca.2020.12.012
- Sherwood, O. A., Guilderson, T. P., Batista, F. C., Schiff, J. T., and McCarthy, M. D. (2014). Increasing Subtropical North Pacific Ocean Nitrogen Fixation Since the Little Ice Age. *Nature* 505, 78. doi: 10.1038/nature12784
- Smith, C. R., Hoover, D. J., Doan, S. E., Pope, R. H., Demaster, D. J., Dobbs, F. C., et al. (1996). Phytodetritus at the Abyssal Seafloor Across 10 of Latitude in the Central Equatorial Pacific. *Deep. Sea. Res. Part II: Top. Stud. Oceanograph.* 43, 1309–1338. doi: 10.1016/0967-0645(96)00015-X
- Takano, Y., Kashiyama, Y., Ogawa, N. O., Chikaraishi, Y., and Ohkouchi, N. (2010). Isolation and Desalting With Cation-Exchange Chromatography for Compound-Specific Nitrogen Isotope Analysis of Amino Acids: Application to Biogeochemical Samples. *Rapid Commun. Mass. Spectromet.* 24, 2317–2323. doi: 10.1002/rcm.4651
- Taylor, S. R., and McLennan, S. M. (1985). *The Continental Crust: Its Composition and Evolution*. New Jersey: Blackwell Scientific Publications.
- Van Der Jagt, H., Wiedmann, I., Hildebrandt, N., Niehoff, B., and Iversen, M. H. (2020). Aggregate Feeding by the Copepods *Calanus* and *Pseudocalanus* Controls Carbon Flux Attenuation in the Arctic Shelf Sea During the Productive Period. *Front. Marine Sci.* 7, 543124. doi: 10.3389/fmars.2020.543124
- Vandewiele, S., Cowie, G., Soetaert, K., and Middelburg, J. J. (2009). Amino Acid Biogeochemistry and Organic Matter Degradation State Across the Pakistan Margin Oxygen Minimum Zone. *Deep. Sea. Res. Part II: Top. Stud. Oceanograph.* 56, 376–392. doi: 10.1016/j.dsr2.2008.05.035
- Yamada, K., Ishizaka, J., and Nagata, H. (2005). Spatial and Temporal Variability of Satellite Primary Production in the Japan Sea From 1998 to 2002. *J. Oceanograph.* 61, 857–869. doi: 10.1007/s10872-006-0005-2
- Yamaguchi, Y. T., Chikaraishi, Y., Takano, Y., Ogawa, N. O., Imachi, H., Yokoyama, Y., et al. (2017). Fractionation of Nitrogen Isotopes During Amino Acid Metabolism in Heterotrophic and Chemolithoautotrophic Microbes Across Eukarya, Bacteria, and Archaea: Effects of Nitrogen Sources and Metabolic Pathways. *Organic. Geochem.* 111, 101–112. doi: 10.1016/j.orggeochem.2017.04.004
- Yamaguchi, Y. T., and McCarthy, M. D. (2018). Sources and Transformation of Dissolved and Particulate Organic Nitrogen in the North Pacific Subtropical Gyre Indicated by Compound-Specific  $\delta^{15}\text{N}$  Analysis of Amino Acids. *Geochim. Cosmochim. Acta* 220, 329–347. doi: 10.1016/j.gca.2017.07.036
- Yang, E. J., Kang, H.-K., Yoo, S., and Hyun, J.-H. (2009). Contribution of Auto-And Heterotrophic Protozoa to the Diet of Copepods in the Ulleung Basin, East Sea/Japan Sea. *J. Plankton. Res.* 31, 647–659. doi: 10.1093/plankt/fbp014
- Yan, G., and Kim, G. (2015). Sources and Fluxes of Organic Nitrogen in Precipitation Over the Southern East Sea/Sea of Japan. *Atmosph. Chem. Phys.* 15, 2761–2774. doi: 10.5194/acp-15-2761-2015
- Yoo, S., and Park, J. (2009). Why is the Southwest the Most Productive Region of the East Sea/Sea of Japan? *J. Marine Syst.* 78, 301–315. doi: 10.1016/j.jmarsys.2009.02.014

**Conflict of Interest:** The authors declare that the research was conducted in the absence of any commercial or financial relationships that could be construed as a potential conflict of interest.

**Publisher’s Note:** All claims expressed in this article are solely those of the authors and do not necessarily represent those of their affiliated organizations, or those of the publisher, the editors and the reviewers. Any product that may be evaluated in this article, or claim that may be made by its manufacturer, is not guaranteed or endorsed by the publisher.

Copyright © 2022 Choi, Hwang, Ryu, Kim and Shin. This is an open-access article distributed under the terms of the Creative Commons Attribution License (CC BY). The use, distribution or reproduction in other forums is permitted, provided the original author(s) and the copyright owner(s) are credited and that the original publication in this journal is cited, in accordance with accepted academic practice. No use, distribution or reproduction is permitted which does not comply with these terms.